

The Structure Function Working Group Summary*

VLADIMIR CHEKELIAN (SHEKELYAN)

MPIM (Munich) and ITEP (Moscow)

AND

AMANDA COOPER-SARKAR

Oxford University

AND

ROBERT THORNE

Cambridge University †

A summary of the experimental and theoretical presentations in the Structure Function Working Group on the proton and photon unpolarized structure functions is given.

1. Introduction

In this report we summarize new results on lepton-nucleon deep inelastic scattering (DIS) from the fixed target experiments NuTeV and Hermes, and from the ep collider HERA in the range of four-momentum transfer squared, Q^2 , between 0.35 and 30000 GeV². Recent next-to-leading-order (NLO) QCD fits and uncertainties of the parton distribution functions (PDFs) are discussed. In the theory part of this summary, developments in lattice QCD, saturation type effects and colour glass condensates, k_T -factorization, and collinear factorization are surveyed.

* Presented at DIS2002, Cracow, 30 April - 4 May 2002

† Royal Society University Research Fellow

2. DIS results on the proton structure functions

2.1. The first NuTeV results on F_2

The $\nu(\bar{\nu})$ -nucleon cross sections from the NuTeV neutrino experiment were presented by R. Bernstein [1]. In Fig.1 (left) the results are compared with the former CCFR data [2] as function of the inelasticity y . The measurements are in a good agreement apart from $x = 0.45$ where the $\bar{\nu}$ results of CCFR are systematically lower. In contrast to CCFR the NuTeV experiment uses very clean ν and $\bar{\nu}$ beams provided by a Sign Selected Quadrupole Train where the charge of the parent π, K of the neutrinos can be selected. The admixtures of the wrong neutrino type is $3 \cdot 10^{-4}$ for ν and $4 \cdot 10^{-3}$ for $\bar{\nu}$ beams. The energy scale uncertainties for muons and hadrons are also improved compared to CCFR with 0.8% for muon (goal 0.3%) and 0.4% for hadrons. For CCFR both uncertainties were 1%.

The sum of ν and $\bar{\nu}$ cross sections depends on F_2 , R , the ratio σ_L/σ_T of longitudinal to transverse cross sections, and $\Delta xF_3 = xF_3^\nu - xF_3^{\bar{\nu}} = 4x(s-c)$ which is sensitive to heavy quark densities. All three functions cannot be derived from the data simultaneously because of strong correlations among corresponding parameters. The first NuTeV results on $F_2(x, Q^2)$, shown in Fig.1 (right), were obtained using the world knowledge on R and ΔxF_3 deduced from the y dependence of the cross sections.

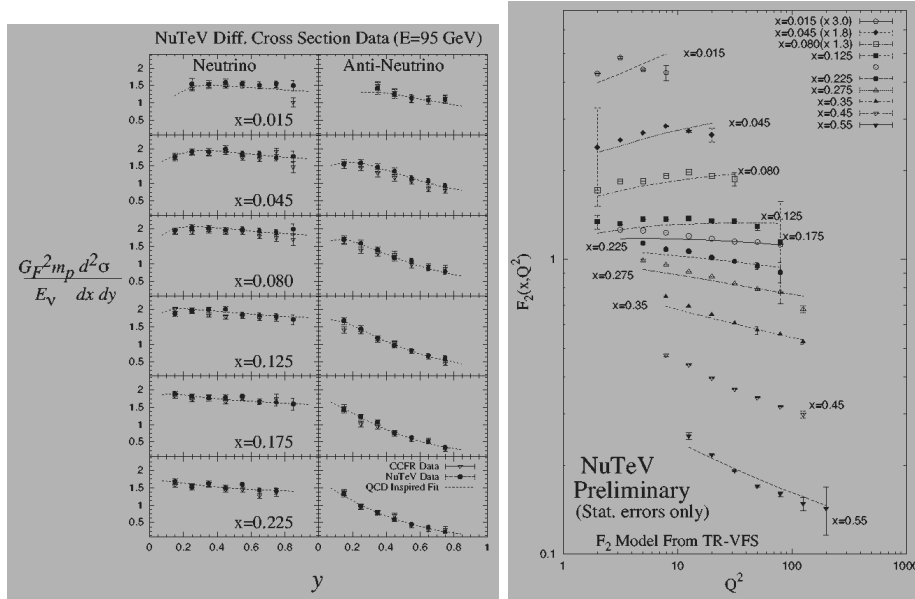


Fig. 1. $\nu(\bar{\nu})$ -nucleon cross sections (left) and $F_2(x, Q^2)$ (right) from NuTeV.

2.2. New HERMES results on nuclear effects in DIS

DIS cross section ratios for positrons of 27.5 GeV on helium-3, nitrogen and krypton with respect to deuterium were measured by the HERMES collaboration (presented by A. Bruell [3]). The helium-3 and nitrogen data were already published [4]. Recently, those data were found to suffer from an A-dependent tracking efficiency of the HERMES spectrometer, which was not recognised in the previous analysis. The resulting correction of the cross section ratios is significant at low values of x and Q^2 and substantially changes the interpretation of those data. The data corrected for this effect are shown in Fig.2. They are in agreement with previous measurements of NMC and SLAC. Values for the ratio R_A/R_D have been derived from the the y dependence of the data and are found to be consistent with unity.

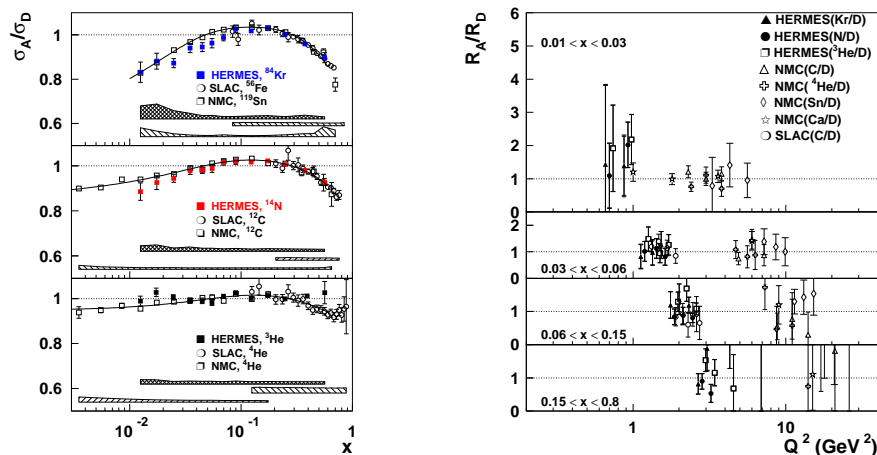


Fig. 2. Ratio of isoscalar DIS Born cross sections for several nuclei with respect to deuterium (left), ratio R_A/R_D (right).

2.3. HERA results at low and medium Q^2

T. Lastovicka [5] presented new H1 data on $F_2(x, Q^2)$ at very low x and $0.35 < Q^2 < 3.5$ GeV 2 in the transition region from the non-perturbative QCD to the DIS domain, see Fig.3. The data were taken in 2000 in a special run with the interaction vertex shifted by 70 cm in the proton beam direction, thereby accessing lower Q^2 than at the nominal vertex position. The luminosity was increased by about a factor of four as compared to the initial shifted vertex run in 1995 which lead to the first H1 [6] and ZEUS [7] data on the proton structure function in the low Q^2 domain.

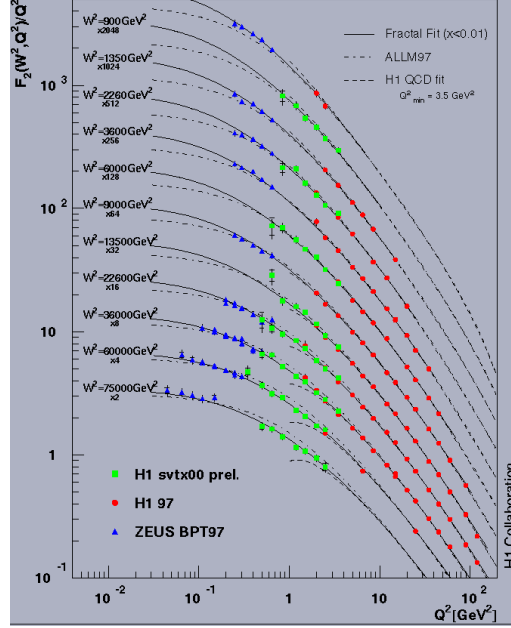


Fig. 3. $F_2/Q^2 \sim \sigma_{tot}(\gamma^*p)$ as function of Q^2 for different W , the invariant mass of the hadronic final state. Grey squares at $0.35 < Q^2 < 3.5 \text{ GeV}^2$ correspond to the new H1 results.

The step rise of the proton structure function F_2 towards small x was first observed in 1993 in the HERA data [8]. In perturbative QCD this rise corresponds to an increase of the gluon density and is expected to slow down at highest energies (small x) due to gluon-gluon interactions. Meanwhile the precision of the F_2 data is much improved and the rise is studied in great detail. J. Gayler [9] presented the local derivative $\lambda = -(\partial \ln F_2 / \partial \ln x)_{Q^2}$ based on the new H1 F_2 data [5] and published precision H1 data [10]. The x and Q^2 dependence of λ is shown in Fig. 4 (left). The derivative is constant for fixed Q^2 in the range $x < 0.01$ consistent with the QCD fit. Therefore the data were fitted assuming the power behaviour $F_2 = c(Q^2)x^{-\lambda(Q^2)}$. The results for the λ and c values are presented in Fig. 4 (right). At $Q^2 < 2 \text{ GeV}^2$ the H1 data were combined with data of NMC [11] and ZEUS [12]. We can state that no damping effects of the rise of F_2 are visible yet at present energies for $Q^2 > 0.85 \text{ GeV}^2$. For $Q^2 \geq 3.5 \text{ GeV}^2$ and $x < 0.01$, F_2 can be well described by the very simple parameterisation $F_2 = cx^{-\lambda(Q^2)}$ with $c \approx 0.18$ and $\lambda(Q^2) = a \cdot \ln(Q^2/\Lambda^2)$. At very low Q^2 λ is approaching 0.08 which corresponds to the energy dependence of soft hadronic interactions

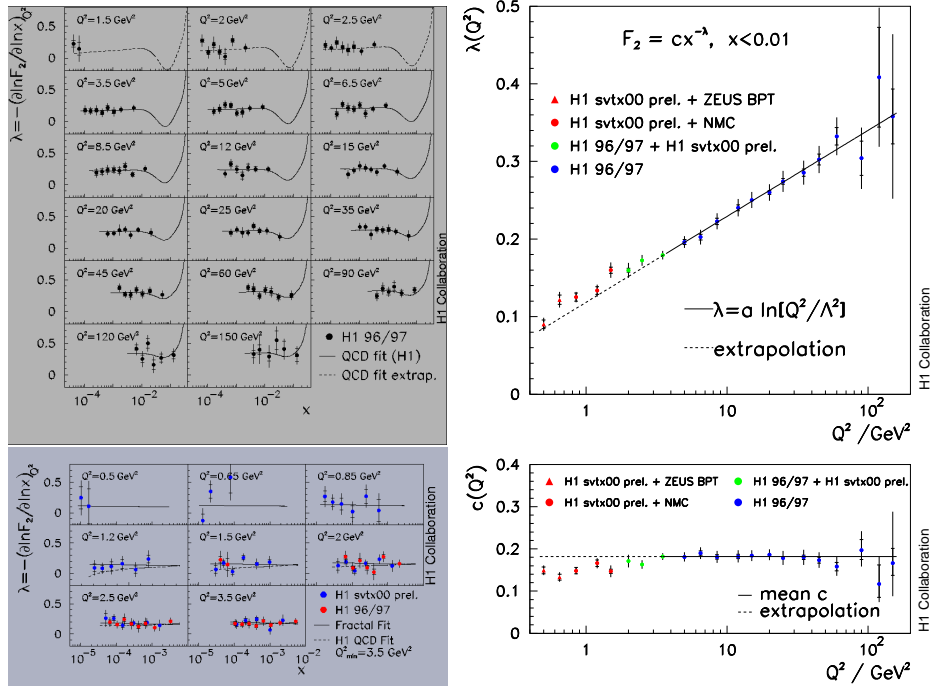


Fig. 4. Local derivative $\lambda = -(\partial \ln F_2 / \partial \ln x)_{Q^2}$ (left) and fitted values of $\lambda(Q^2)$ and $c(Q^2)$ (right).

$$\sigma_{tot} \sim s^{\alpha_P(0)-1} \approx s^{0.08} [13].$$

2.4. High Q^2 HERA data

New high Q^2 HERA data were presented by M. Ellerbrock [14], M. Moritz [15] and S. Griepink [16]. Both ZEUS and H1 have results from $\sim 16 \text{pb}^{-1}$ of e^-p data taken in the years 1998-1999 and $\sim 60 \text{pb}^{-1}$ of e^+p data taken in the years 1999-2000, both at $\sqrt{s} = 318 \text{GeV}$. These e^+p data can be combined with the previously published data at $\sqrt{s} = 300 \text{GeV}$ to give a total sample of $\sim 90 \text{pb}^{-1}$.

The ZEUS and H1 data for neutral (NC) and charged current (CC) $e^\pm p$ scattering are compared in Fig. 5. There is excellent agreement between the experiments and with the Standard Model predictions for electroweak unification at high Q^2 .

Neglecting the small contribution of F_L , the differential cross-section for

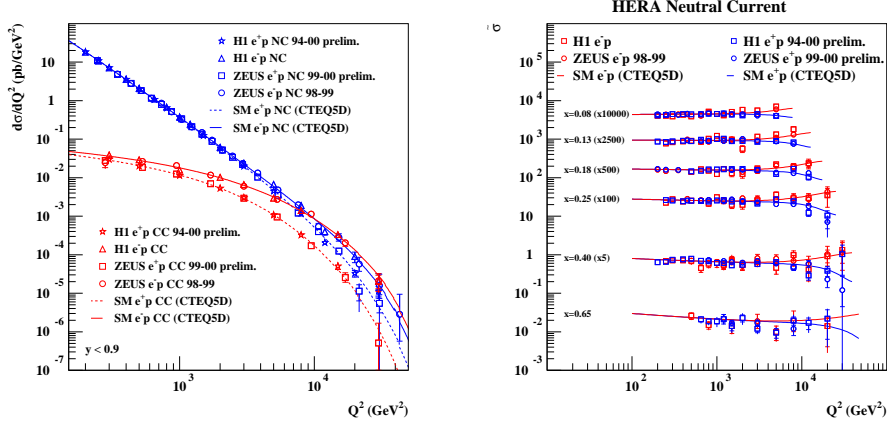


Fig. 5. Comparison of the ZEUS/H1 data on $e^\pm p$ CC and NC scattering (left). The NC e^\pm reduced cross-sections as a function of Q^2 (right).

NC $e^\pm p$ scattering is given by

$$\frac{d^2\sigma(e^\pm p)}{dx dQ^2} = \frac{2\pi\alpha^2}{Q^4 x} [Y_+ F_2(x, Q^2) \mp Y_- xF_3(x, Q^2)], \quad (1)$$

where F_2, xF_3 are expressed in terms of parton distribution functions (PDFs) as

$$F_2(x, Q^2) = \sum_i A_i(Q^2)(xq_i(x, Q^2) + x\bar{q}_i(x, Q^2)) \quad (2)$$

and

$$xF_3(x, Q^2) = \sum_i B_i(Q^2)(xq_i(x, Q^2) - x\bar{q}_i(x, Q^2)) \quad (3)$$

in leading order perturbative QCD. For unpolarised lepton beams the coefficients A, B are given in terms of electroweak couplings [18]. The parity violating structure function xF_3 is only significant at high Q^2 . Fig 5 also shows the difference in the e^+ and e^- NC cross-sections due to this xF_3 term as a function of Q^2 . This has been used to extract xF_3 and a new measurement from ZEUS is shown in Fig 6. With the greater luminosity of HERA-II a precision measurement of this valence structure function will be possible across all x . Currently the only such precision measurement is the xF_3 measurement from CCFR $\nu, \bar{\nu}$ scattering on an Fe target.

High Q^2 CC data can be used to gain information on the high x valence PDFs, with flavour separation between u_v and d_v . CC scattering involves only the quark flavours which are appropriate to the charge of the current, so that the differential cross-section for CC $e^\pm p$ scattering with unpolarized

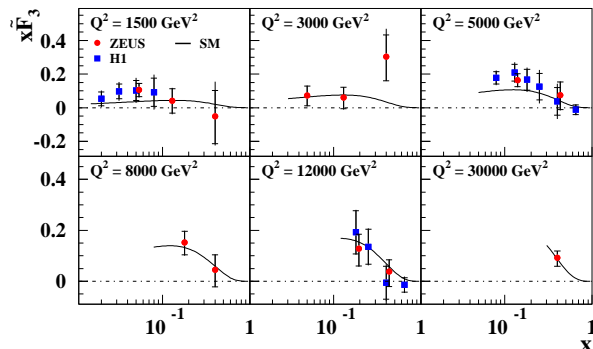


Fig. 6. The structure function xF_3 extracted from ZEUS high Q^2 NC $e^\pm p$ data.

beams is given by

$$\frac{d^2\sigma(e^-p)}{dx dQ^2} = \frac{G_F^2}{2\pi x} \frac{M_W^4}{(Q^2 + M_W^2)^2} \left[xU(x, Q^2) + (1-y)^2 x\bar{D}(x, Q^2) \right] \quad (4)$$

and

$$\frac{d^2\sigma(e^+p)}{dx dQ^2} = \frac{G_F^2}{2\pi x} \frac{M_W^4}{(Q^2 + M_W^2)^2} \left[x\bar{U}(x, Q^2) + (1-y)^2 xD(x, Q^2) \right] \quad (5)$$

where U stands for U -type quarks with charge $+2/3$ and D for D -type quarks with charge $-1/3$. Clearly at high x the e^-p cross-section is dominated by the u_v PDF and the e^+p cross-section by the d_v PDF. The new high Q^2 CC data are shown in Fig 7. Their contribution to the precision extraction of PDFs will be discussed in Sec. 3.2.

The strong dependence of the CC cross-sections on the W propagator can be used to make an extraction of M_W in a space-like process. The results from ZEUS and H1 for e^- and e^+ data are given in Table 1. The e^- data give the better determinations, both because of the larger cross-section and because of the reduced uncertainty from the PDFs when the better known u quark distribution is dominant.

At HERA-II our ability to measure electroweak parameters will be greatly improved both due to increased statistics and due to the polarization of the beams, as detailed in the contribution of F. Metlica [17]. For example, with $1fb^{-1}$ and $P(e^-) = -0.7$, the error achievable will be $\Delta M_W \sim 0.055\text{GeV}$, c.f. the PDG value $\Delta M_W \sim 0.049\text{GeV}$ from time-like processes.

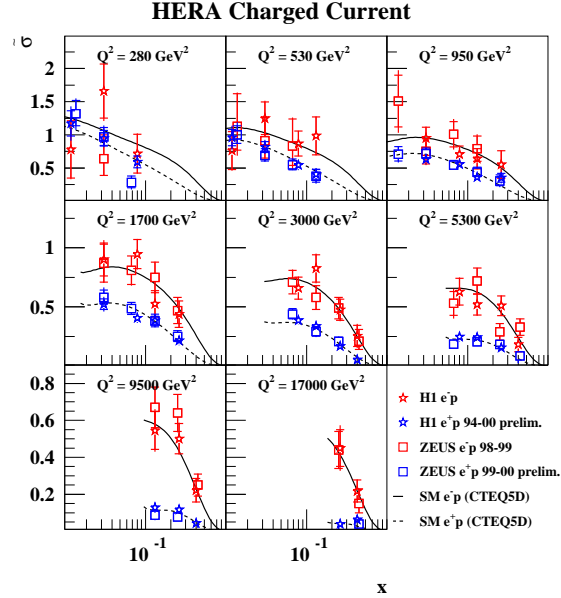


Fig. 7. $CC e^\pm p$ data from ZEUS and H1

Experiment	beam	M_W
ZEUS	e^+	$81.4 \pm 2.7(\text{stat}) \pm 2.0(\text{sys}) \pm 3.0(\text{PDF})$
H1	e^+	$80.9 \pm 3.3(\text{stat}) \pm 1.7(\text{sys}) \pm 3.7(\text{PDF})$
ZEUS	e^-	$80.3 \pm 2.1(\text{stat}) \pm 1.2(\text{sys}) \pm 1.0(\text{PDF})$
H1	e^-	$79.9 \pm 2.2(\text{stat}) \pm 0.9(\text{sys}) \pm 2.1(\text{PDF})$

Table 1. Values of M_W extracted from ZEUS and H1 CC data

3. Recent NLO QCD fits

A large amount of new data has become available during the past couple of years, in particular the recent measurements of inclusive DIS cross sections in ep interactions by H1 and ZEUS and the inclusive high- E_T jet data by D0 and CDF. The improved precision of the data led to a new generation of global NLO DGLAP QCD analyses, such as MRST01 [19] and CTEQ6 [20] presented at the workshop by R. Thorne [21] and W.K. Tung [22]. B. Reisert [23] and E. Tassi [24] presented QCD fits performed by H1 [10] and ZEUS using their respective data supplemented by the data from fixed target experiments. Improved quality of the fits is achieved due to more precise data as well as due to a new level of sophistication in the

fitting technique including a full treatment of available experimental correlated systematic uncertainties.

The MRST01, CTEQ6 and ZEUS PDFs are compared in Fig. 8, where the error band illustrated is that from the ZEUS standard (ZEUS-S) analysis. There is good agreement of all these PDFs within experimental uncertainties.

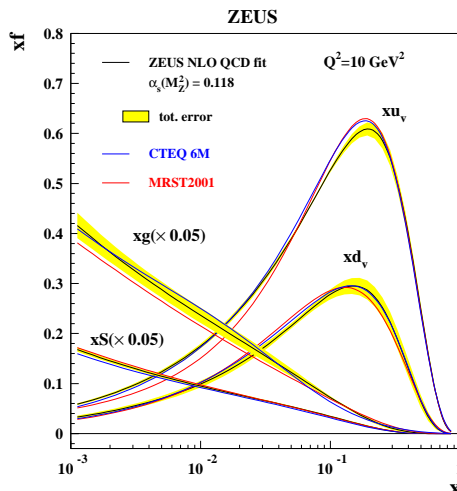


Fig. 8. Comparison of the ZEUS, MRST2001 and CTEQ6 PDFs. The error band is that of the ZEUS standard (ZEUS-S) global fit.

3.1. Uncertainty of parton distributions from QCD fits

A new feature of the recent QCD analyses is a systematic and pragmatic treatment of the uncertainties of the parton distribution functions and their physical predictions. One of the problems of the uncertainty estimation for fits with many data sets is related to a certain degree of inconsistency of the latter. Usually the one sigma error of a parameter in a fit is determined by variation of χ^2 by one unit from the minimum. Very often, however, this rule becomes unrealistic. This is demonstrated in Fig. 9, where the distances from χ^2 -minima of individual data sets to the global minimum by far exceeds the range allowed by the $\Delta\chi^2 = 1$ criterion. It is not possible to simply drop “inconsistent” data sets, as then the partons in some regions would lose important constraints. On the other hand the level of “inconsistency” should be reflected in the uncertainties of the PDFs. This can be achieved by modification of the χ^2 tolerance criterion to $\Delta\chi^2 = T^2$ [20, 19, 25, 26] where T stands for a tolerance which should be estimated from the level of (in)consistency of the data sets used in each particular QCD fit. In the

CTEQ6	$\Delta\chi^2 = 100$	$\alpha_s(M_Z^2) =$	$0.1165 \pm 0.0065(exp)$
ZEUS	$\Delta\chi_{eff}^2 = 50$	$\alpha_s(M_Z^2) =$	$0.1166 \pm 0.0049(exp)$
			$\pm 0.0018(model) \pm 0.004(theory)$
MRST01	$\Delta\chi^2 = 20$	$\alpha_s(M_Z^2) =$	$0.1190 \pm 0.002(exp) \pm 0.003(theory)$
H1	$\Delta\chi^2 = 1$	$\alpha_s(M_Z^2) =$	$0.115 \pm 0.0017(exp)$
			$+ 0.0009 (model) \pm 0.005(theory)$
			$- 0.0005 (model) \pm 0.005(theory)$

Table 2. Values of $\alpha_s(M_Z^2)$ and its error from different NLO QCD fits with different error tolerances.

CTEQ6 fit the tolerance was taken to be 10 ($\Delta\chi^2 = 100$), as shown by the horizontal lines in Fig. 9 (right). The choices for T^2 in the QCD fits are listed in Table 2 and range from 1 to 100.

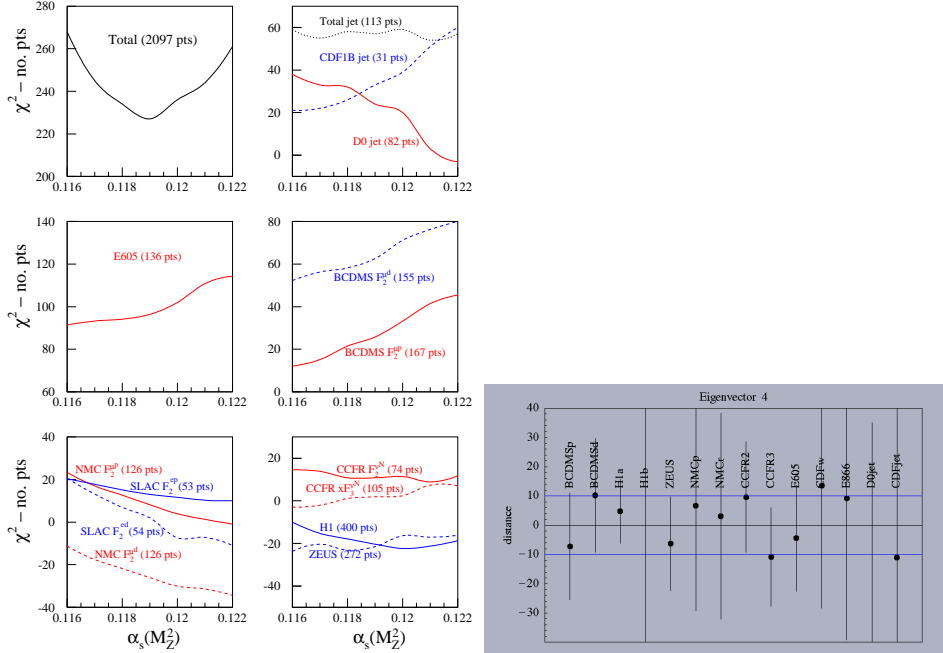


Fig. 9. Partial χ^2 for data sets in the MRST01 fit as function of $\alpha_s(M_Z^2)$ (left). Distance along a parameter combination (eigenvalue 4, CTEQ6) from the χ^2 -minimum of an individual data set to the global minimum (right). In the neighborhood of the global minimum a distance of 1 corresponds to $\Delta\chi_{global}^2 \approx 1$.

The values of the strong coupling constant $\alpha_s(M_Z^2)$ obtained in the fits are also given in Table 2. They are remarkably consistent. However, the

estimates of the experimental uncertainties on $\alpha_s(M_Z^2)$ are different due to different judgements on the $\Delta\chi^2$ criterion. This is not a contradiction, all choices are legitimate and reflect different emphases in the fits. For example, H1 [10] uses the canonical $\Delta\chi^2 = 1$ after careful consistency checks of the two data sets (H1 and BCDMS μp) used in the fit. The relative uncertainty bands for the gluon distribution obtained in the CTEQ6 and ZEUS-S fits are shown in Fig. 10. They illustrate a reasonable consistency of judgement on the experimental errors of the gluon PDF.

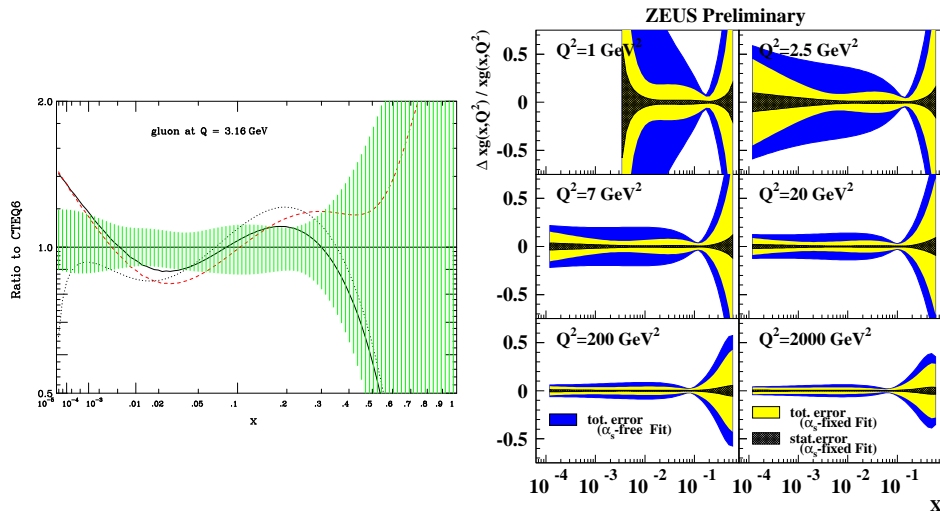


Fig. 10. Relative gluon uncertainties as determined in the CTEQ6 fit (left) and the ZEUS-S QCD fit (right).

Thus, there are reasonable approaches to how to treat experimental statistical and systematical errors, how to take into account model uncertainties such as charm or bottom masses, and how to account for incompatibilities of data sets. It is not so easy to estimate theoretical uncertainties, this is explored further in [21] and in Sec. 5.4. The model uncertainty which comes from the choice of parametric forms for the PDFs at the input scale also merits further investigation. The latter issue was studied by CTEQ [20] and H1. B. Reiser [23] presented an investigation of the parameter space using general forms of MRST type parameterisations $x \cdot PDF = ax^b(1-x)^c(1+d\sqrt{x}+ex)$ for the PDFs of the gluon, quarks and anti-quarks at the input scale. Starting with the parameters a, b, c for each PDF, an additional parameter was considered only when its introduction improved χ^2 by more than one unit. The uncertainty envelope in this study was defined as an overlap of the experimental and model error bands of fits

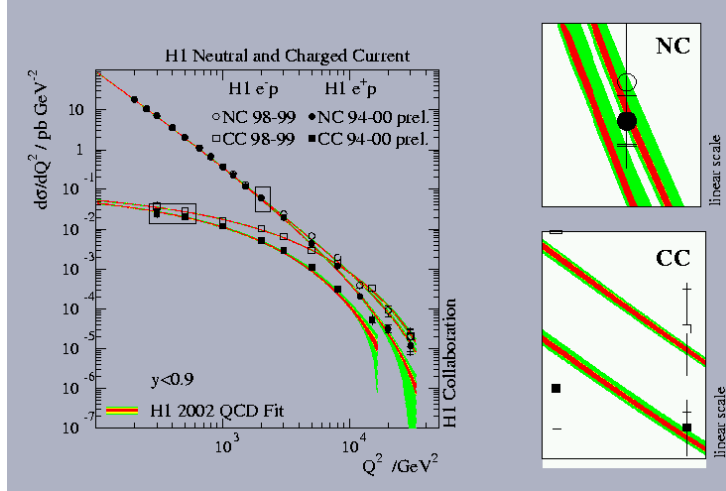


Fig. 11. Single differential cross sections $d\sigma/dQ^2$ for NC and CC processes in the $e^\pm p$ interactions (left). Grey error bands are envelopes of the QCD fit results corresponding to variations of parametric forms. The boxes in the left figure for NC and CC at moderate Q^2 are zoomed and shown on the right.

with $\chi^2 < \chi_{best}^2 + \sqrt{2N_{dof}}$. Here χ_{best}^2 corresponds to the fit with the best χ^2 . This criterion is constructed by analogy with the statistical error of χ^2 . It is somewhat arbitrary and used here only provisionally. The uncertainty bands in Fig. 11 show that an assumption on the parametric form for the PDFs at an input scale of $Q_0^2 = 4 \text{ GeV}^2$ influences the predictions of the QCD fit even at moderate Q^2 in the case of highly integrated observables like $d\sigma/dQ^2$.

3.2. Results from QCD fits

The HERA data are crucial for determining the low x sea and gluon shapes. The ZEUS-S sea and gluon distributions are compared in Fig 12 [24]. The gluon density is much larger than the sea density for $Q^2 > 5 \text{ GeV}^2$, but for lower Q^2 the sea density continues to rise at low x (consistent with the rise in F_2 down to low Q^2 mentioned in Sec 2.3), whereas the gluon density is suppressed. This could be a signal that the conventional DGLAP formulation of NLO-QCD is inadequate in this region. Fig. 12 also shows data at very low Q^2 compared to the ZEUS-S fit. Such a fit clearly fails for $Q^2 \leq 0.65 \text{ GeV}^2$, even when the conservative error bands on the fit are considered.

For this generation of PDFs the data which most strongly determine

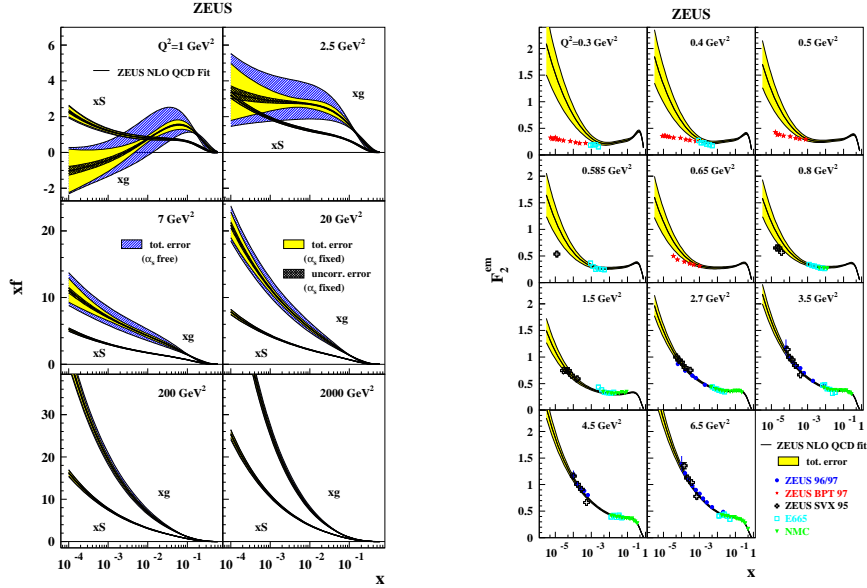


Fig. 12. Gluon and sea distributions for the ZEUS-S fit (left). F_2 data at very low Q^2 compared to the ZEUS-S fit. (right).

the valence distributions are the fixed target data. However new high Q^2 HERA data can put some constraint on the valence distributions and this is important because these data do not suffer from the uncertainties associated with nuclear target corrections.

Both the NC and CC high- Q^2 data are very well described by the global PDF fits. ZEUS has also made a special fit to ZEUS data alone (ZEUS-O) including the new e^-p 98/99 and the preliminary e^+p 99/00 high Q^2 data [24]. In this fit these additional data sets were used instead of the fixed-target data to constrain the valence distributions. Fig. 13 compares the valence distributions from the ZEUS-S global fit to those for the ZEUS-O fit. The level of precision of the ZEUS-O fit is approaching that of the global fit and its precision is statistics limited rather than systematics limited, so that improvement can be expected with higher luminosity HERA-II data. The systematic precision of high- x ($x > 0.7$) measurements at HERA-II can also be improved further as explored in the contribution of M. Helbich [27].

There are further advantages to using HERA data alone. In the ZEUS-O fit, the high- x d -valence distribution is determined by the high- Q^2 e^+p CC data. In contrast in the global fits it is strongly determined by the NMC

F_2^D/F_2^p data. It has been suggested that such measurements are subject to significant uncertainty from deuteron binding corrections [28]. The ZEUS-O extraction does not suffer this uncertainty.

The ZEUS-O fit was made using the same form of parton parametrization as the ZEUS-S global fit. For the global fits, parametrization dependence is not severe since, for example, the valence shapes are strongly constrained across all x by the CCFR xF_3 data, and the $\bar{d} - \bar{u}$ distribution is constrained by D, p target data. However, if HERA data alone are used, then these constraints are lost and parametrization dependence can be significant, as discussed in Sec 3.1 [23]. At HERA-II the precision measurement of xF_3 across all x should considerably reduce this uncertainty, and eliminate the uncertainty from heavy target corrections which is unavoidable in the CCFR xF_3 measurement.

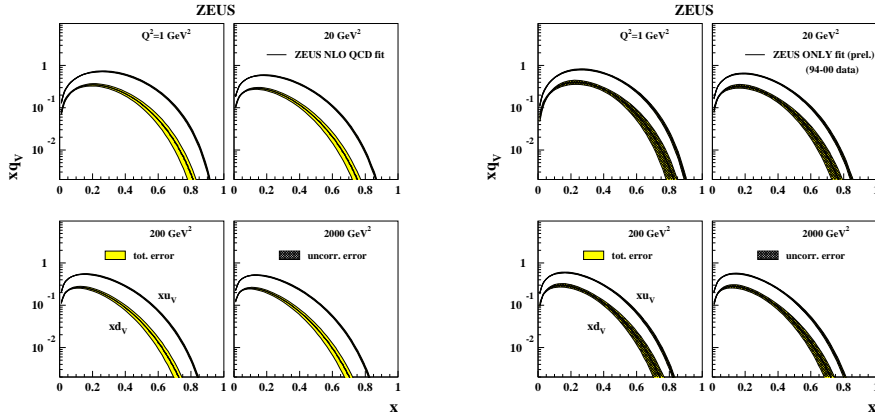


Fig. 13. Valence distributions for the ZEUS-S fit (left). Valence distributions for the ZEUS-O fit (right).

4. $F_2^{c\bar{c}}$, F_2^γ

Results relevant to the charm structure function and the photon structure function were extensively covered in the Hadron Final States Working Group and will not be discussed again in detail here. Results from HERA on the charmed structure function were reviewed for the Structure Function Working Group by O. Behnke [29]. M. Prybycien [30] reviewed the status of photon structure function measurements at LEP.A. De Roeck [31] presented new OPAL data from two-photon processes and S. Maxfield [32] reviewed measurements of real and virtual photon structure. There was also some progress in developing new PDF sets for the photon, accounting for modern

data and correct heavy quark treatment, as presented by S. Albino [33] and P. Jankowski [34].

5. Theory

At this workshop the main emphasis of the theoretical contributions was the different ways in which one can calculate structure functions and the regions of applicability of these different approaches. Essentially there were four alternative methods which were outlined, all of which have seen significant progress, or at least new results. These are:

1. Lattice QCD.
2. Saturation type effects/colour glass condensates.
3. k_T -factorization.
4. Collinear Factorization.

There were also some other talks which do not fall into these general categories. D. Haidt presented a consistency check for DGLAP evolution [35], examining the partons extracted from the measured values of F_2 and $dF_2/d\ln Q^2$ and checking that these are consistent with the evolution equations. A discrepancy is found at low x and Q^2 . T. Lastovicka demonstrated that a good fit to structure functions may be obtained using a parameterization determined by assuming a self similar structure, i.e. using the fractal dimensions for the structure functions [36]. A. Kotikov presented a fit to high x data using cuts determined by the region of large systematic errors extracting, for example, $\alpha_S(M_Z^2) = 0.1174 \pm 0.0007(\text{stat}) \pm 0.0019(\text{sys}) \pm 0.0010(\text{norm})$ from a nonsinglet fit [37]. D. Timashkov also presented an analytic formula for structure functions for all x and Q^2 based on expressions in the limiting cases $Q^2 \rightarrow 0$, $x \rightarrow 1$ and $x \rightarrow 0$ [38]. However, the summary is based on the above four alternative procedures.

5.1. Lattice QCD

There has been significant progress in this area, and we were given a summary by S. Capitani [39]. It is not possible to compute structure functions directly on the lattice because the parton distributions are defined on the light cone, while lattice simulations are done in Euclidean space. However, one can use the Operator Product Expansion and calculate moments. The main effort has been in the calculation of 1st, 2nd and 3rd moments of nonsinglet distributions, both for unpolarized and polarized structure functions. A reason for only calculating nonsinglet quantities is due to the difficulty in computing disconnected diagrams (i.e., connected only by gluon lines) due to the expense in computer time. Nonsinglet quantities are insensitive to such diagrams.

One of the main improvements has been the first calculations without using the quenching approximation. This has shown that, for nonsinglet quantities at least, the quenched approximation is indeed very good. There have also been improvements in the perturbative renormalization factors required to translate the results on the lattice to a particular continuum renormalization scheme (e.g. $\overline{\text{MS}}$). In order to obtain the final results on the lattice it is ultimately necessary to perform chiral and continuum extrapolations, using a fit formula $A + Bm_\pi^2 + ca^2$, due to the finite lattice spacing a and to the fact that one currently has a pion with mass $m_\pi \sim 500\text{MeV}$. This appears to be well under control, but the results are disappointing – for the first moment of the $u - d$ distribution they find 0.30 ± 0.03 where the standard distributions give 0.23 ± 0.02 . The results for polarized distributions are more in agreement with experiment.

It is thought that this discrepancy is due to the finite size of the lattice missing the effects of the pion cloud. From chiral perturbation theory one obtains terms $\sim m_\pi^2 \ln m_\pi^2$. Introducing an additional term in the extrapolation formula of the form $m_\pi^2 \ln(m_\pi^2/\Lambda^2)$ can solve this problem, but only for Λ a free parameter $\sim 300 - 700\text{MeV}$ for various processes, destroying any predictive power. One needs lattices such that $m_\pi < 250\text{MeV}$, which may be possible with computers within a couple of years. It would also be desirable to investigate the pion cloud effects by doing simulations with larger physical volumes. Finally, preliminary investigations of higher twist moments have been performed, giving results which are surprisingly small.

5.2. Saturation type effects/colour glass condensates

There was a lot of emphasis on the region of small x and low Q^2 where the gluon density is expected to saturate. Recently a great deal of interest has focused on the GBW saturation model [40]. In this one factorizes deep inelastic scattering into the fluctuation of the virtual photon into a dipole pair and the dipole-proton cross-section. The former is calculable at LO and the latter is modelled in the form

$$\hat{\sigma}(x, r) = \sigma_0 [1 - \exp(-r^2/4R_0^2(x))]$$

where r is the dipole size and $R_0^2(x) = (x/x_0)^\lambda \text{GeV}^{-2}$. This then saturates at large r and low x and predicts geometric scaling, i.e. that the structure functions are functions of $Q^2 R_0^2(x)$ alone. For $\lambda \sim 0.28$ this model could be made to fit data well, and the procedure could then predict the total diffractive cross-section. We had a presentation from N. Timneanu on an extension of this type of approach to two photon physics [41]. Using a number of sensible extensions of the dipole-proton cross-section to model the dipole-dipole cross-section he demonstrated that a good fit to existing

data on photon-photon cross-sections is obtained for both real and virtual photons. However, this data is not very precise, and in particular, can not distinguish between the different extensions.

However, the new more accurate HERA data on proton structure functions presented at this workshop is very precise and forces the simple saturation model to be modified, e.g., the effective power λ in $F_2(x, Q^2) \sim x^{-\lambda}$ is accurately measured to run with Q^2 (see Sec. 2.3 and Fig. 4) whereas it saturates at moderate Q^2 in the simplistic saturation model. In order to rectify this it is necessary to include DGLAP evolution in the model [42], replacing the above $\hat{\sigma}(x, r)$ by

$$\hat{\sigma}(x, r) = \sigma_0 \left[1 - \exp\left(\frac{-\pi^2 r^2 \alpha_s(\mu^2) x g(x, \mu^2)}{3\sigma_0}\right) \right],$$

where μ^2 is parameterized in terms of r^2 . This can improve the fit considerably, as shown in Fig. 14. However, it moves one away from the original principles somewhat, and geometric scaling is violated. There are two alternative formulations in [42] (somewhere between the two is likely to be most realistic), both moving the saturation scale to lower x and Q^2 . Including charm quarks rather than only 3 light flavours in the original model (hardly optional since charm contributes over 30% of the structure function in some regions) also moved the saturation scale down an order of magnitude in x . If this is also true for the modified model it implies that for $Q^2 = 1\text{GeV}^2$ saturation sets in only for $x < 0.00001$ in structure functions.

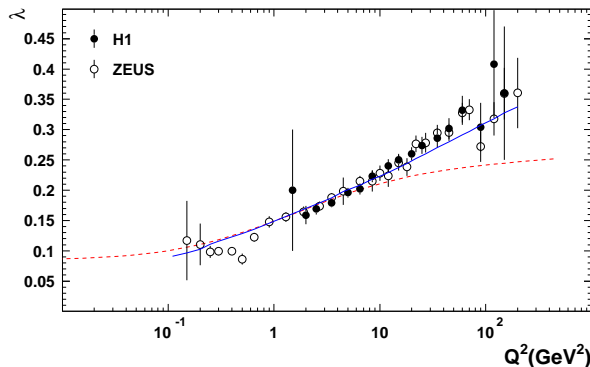


Fig. 14. The effective slope λ as a function of Q^2 - the original saturation model (dashed line) and the improved model (dotted line).

We also had some other talks on saturation in QCD, discussing the solutions to the nonlinear equations describing QCD at high parton density and adding support to the type of models considered above. We had a review of this subject by L. McLerran [43] (which will be discussed in the

summary of the diffractive session). We also had a presentation by A. Freund which outlined some specific points [44]. He told us that “Colour Glass Condensate” simply means that in QCD (colour) at high energies, fields slowly evolve relative to natural scales (glass) and the phase-space density saturates (condensate). Hence, at high energies, but at scales high enough that perturbative QCD applies, one can write a renormalization group equation in x in terms of suitable variables [45]. This results in a Fokker-Plank equation which is nonlinear, but which one can use known techniques to solve. Implementing a single input condition one obtains a solution (for fixed α_S) of the general form $F_2(x, Q^2) = (x/x_0)^{2\lambda} f(x_0, ((\frac{x}{x_0})^\lambda \frac{Q}{Q_0})^2)$ where $\lambda = 0.18$, which fits the data well and is similar to geometric scaling. This has also been applied to nuclear structure functions with successful results, and where it is found that the scaling variable is $Q^2(x/x_0)^{2\lambda} A^{-\delta}$, where $\delta = 0.1$ rather than the naively expected $1/3$. Hence, the first principle solutions in the colour-glass-condensate approach support the saturation models, implying a similar type of scaling. Corrections to this scaling have been estimated. However, there are further improvements to be made, e.g. a full treatment of running coupling, and it is intriguing that geometric scaling should work so well when the charm quark contribution is ignored, despite the fact that it contributes a great deal to the structure function, and should lead to violation of any geometric type scaling.

5.3. k_T factorization

This should be applicable at high energies at scales where perturbation theory holds but high density effects are minimal. There have been a number of improvements in this field. One of these is in the Monte Carlo based on k_T -factorization. H. Jung showed that there has been significant progress in correcting previous shortcomings in the CASCADE Monte Carlo [46], both in the treatment of the scale in the running of the coupling and in the inclusion of the non-singular terms in the $\mathcal{O}(\alpha_S)$ gluon-gluon splitting function [47]. Explicitly, in the original version the splitting function had the form $P = \frac{\bar{\alpha}_S}{1-z} + \frac{\bar{\alpha}_S}{z} \Delta_{ns}$ where Δ_{ns} is the non-Sudakov form factor. This misses the non-singular terms $\bar{\alpha}_S(-2+z(1-z))$ in the LO splitting function. Since this is a negative contribution its omission leads to a bigger gluon at high and moderate x . This has led to the modification

$$P = \bar{\alpha}_S \left(\frac{z}{1-z} + Bz(1-z) \right) + \bar{\alpha}_S \left(\frac{1-z}{z} + (1-B)z(1-z) \right) \Delta_{ns}$$

where $B \sim 0.5$, as well as changes to the form factors. Unfortunately, although these modifications, or something similar, are necessary, the decreased positive contribution to the evolution at moderate x actually leads

to worse agreement with data for forward jets, and Tevatron b production, with the data showing an excess in both cases. There was also an alternative approach to k_T -factorization based Monte Carlos presented by G. Miu [48]. This is based on the Linked-Dipole-Chain model, and differs mainly in the manner in which partons are separated into initial and final state emissions. The resulting integrated gluon distribution obtained from fits to F_2 agree well with standard distributions. While this need not be the case at small x , where k_T -factorization and collinear factorization may well differ, it must be the case at higher x , where a correctly modified Monte Carlo should not significantly alter the conventional results.

A. Stasto talked on solutions to the LO BFKL equation with running coupling [49]. She argued that if one calculates the purely perturbative contribution to the high-energy gluon Green's function one obtains an expansion in $\beta_0 \bar{\alpha}_S^2 Y$ which is reasonably well-behaved as long as $\beta_0 \bar{\alpha}_S^2 Y \leq 0.1$ (beyond this the series diverges), and explicit results are known for this series [50]. It was also demonstrated that the transition to the nonperturbative region is a sudden tunneling-like effect, rather than due to diffusion as is generally assumed [51]. The regime where the alternative methods of breakdown occur was compared and found to be similar for $\bar{\alpha}_S \leq 0.1$ but the perturbative expansion having a larger range of applicability for lower $\bar{\alpha}_S$ (or in the formal limit of small β_0). However, $\beta_0 \bar{\alpha}_S^2 Y \leq 0.1$ is not in practice a very wide range, and it is unclear if purely perturbative calculations of high-energy scattering are really possible in a quantitative sense, though higher order corrections may help matters.

S. Gieseke presented an update of the present status of the calculation of NLO impact factors in the BFKL framework [52]. This consists of two different contributions - the one-loop virtual corrections to the quark box diagrams and the contributions with an additional gluon in the intermediate state, as illustrated in Fig. 15. The calculation of the vertex diagrams in each of these two cases is now complete, and moreover, it has been proven that the infrared divergences due to the two separate contributions cancel each other in the appropriate manner. However, it still remains to perform the integrals over phase space to obtain the final result. Once this is done we will finally be in a position where NLO calculations of physical processes can be made with the k_T -factorization framework for the first time.

5.4. Collinear factorization

This is what we normally think of as standard perturbative QCD, which we use assuming high accuracy at large scales and uncertain x , usually at NLO. Within the framework of NLO QCD, S. Kretzer gave a presentation of various issues in heavy-flavour production [53]: a prescription for fully differential charm production at NLO for charm production in DIS [54], which will be important in determining the strange quark distribution with more

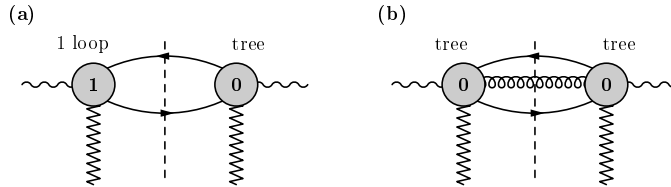


Fig. 15. Contributions to the γ^* impact factor.

accuracy at NuTeV; the NLO and mass corrections to the DIS contribution to $\nu_\tau N \rightarrow \tau X$; and a modification of the ACOT prescription for inclusive charm production in DIS to include the appropriate threshold behaviour in coefficient functions at each order [55]. J. Bartels also gave a summary of the contribution of higher twist operators at small x [56]. Within the context of the double-leading-log approximation, and having to model the inputs, the contributions of the four sources due to gluon operators show a potentially large cancellation in F_2 , but imply a large negative twist four correction to F_L .

S. Moch gave a summary of NNLO calculations of splitting functions and coefficient functions [57]. These rely on calculating the Mellin moments of the structure functions, which results in simplification since internal propagators in diagrams which depend on the parton momentum p can be expanded in powers of $(p \cdot q/q^2)^N$ where N indeed corresponds to the Mellin moment variable. For the diagrams with only one internal line dependent on p , known as basic building blocks, this reduces 4-point diagrams to 2-point diagrams and the calculation is greatly simplified. Various techniques then also have to be used to relate more complicated diagrams to these building blocks [58]. A number of fixed moments of 3-loop splitting functions and coefficient functions have already been calculated [59]. The complete calculation of non-singlet quantities is nearly finished. The much more complicated singlet quantities will be a little longer.

Finally, we had an update on both the MRST and CTEQ parton distributions [19, 20]. W.K.Tung [22] concentrated on the treatment of uncertainties due to experimental errors (discussed in Sec. 3.1). R. Thorne [21] instead emphasized the need to understand theory errors for partons as well as the development of experimental errors. For example, MRST have used the approximate NNLO splitting functions in [62] to perform global fits and make predictions at NNLO [61]. This suggests that NNLO leads to a bigger correction even to the W cross-section at Tevatron than the experimental error within NLO. The theory errors associated with higher orders are probably much bigger for gluon dominated quantities. Additionally, detailed investigation of cuts on data [60] suggest that the fits improve if the lowest Q^2 and particularly lowest x data are cut out, and the predictions

for cross-sections with the new partons change. This suggests potentially large corrections to NLO DGLAP at low Q^2 and low x .

5.5. Theoretical Conclusions

As outlined, there are various different approaches to calculating structure functions, and there has been real progress in some of these calculations, e.g. NNLO in the usual expansion in α_S , in the colour glass model and in NLO corrections to BFKL impact factors. All the approaches are probably applicable in their own regime, and in some cases can be extrapolated with considerable success for surprising distances. However, this success may sometimes lead to unwarranted claims that one approach is actually particularly appropriate. There needs to be more real understanding of precisely where the regimes are and how they can be combined in order to produce the best overall theory with the maximum predictive power. In our opinion the best theory, particularly when one considers the predictive power for a wide range of processes over a range of different experiments (HERA, Tevatron, NuTeV, LEP, LHC) is probably the collinear factorization theorem, but improved as much as possible by, for example, resummations at small and large x , higher twist corrections, etc. Clearly this will then require modification in the nonperturbative regime. This construction of the best complete, universally applicable theory is a difficult task, and help will be needed from even more precise and wide-ranging data.

6. Conclusions

New precise results on structure functions across a wide range of Q^2 , from 0.35 to 30000GeV², have been presented this year. The data are now systematics rather than statistics limited such that QCD fits to extract parton distributions and α_s have to consider correlated systematic errors. The precision of the data requires extension of the conventional formalism of NLO QCD, as embodied in the DGLAP formalism, and this challenge is being met as this formalism extended in various directions: to NNLO, to small x , to high density and to the non-perturbative regime.

REFERENCES

- [1] R. Bernstein, these proceedings.
- [2] U. K. Yang *et al.* [CCFR/NuTeV Collaboration], Phys. Rev. Lett. **86** (2001) 2742.
- [3] A. Bruell, these proceedings.
- [4] K. Ackerstaff *et al.* [HERMES Collaboration], Phys. Lett. B **475** (2000) 386.

- [5] T. Lastovicka, these proceedings.
- [6] C. Adloff *et al.* [H1 Collaboration], Nucl. Phys. B **497** (1997) 3.
- [7] J. Breitweg *et al.* [ZEUS Collaboration], Eur. Phys. J. C **7** (1999) 609.
- [8] I. Abt *et al.* [H1 Collaboration], Nucl. Phys. B **407** (1993) 515;
M. Derrick *et al.* [ZEUS Collaboration], Phys. Lett. B **316** (1993) 412.
- [9] J. Gayler, these proceedings and hep-ex/0206062; C. Adloff *et al.* [H1 Collaboration], Phys. Lett. B **520** (2001) 183.
- [10] C. Adloff *et al.* [H1 Collaboration], Eur. Phys. J. C **21** (2001) 33.
- [11] M. Arneodo *et al.* [New Muon Collaboration.], Phys. Lett. B **364** (1995) 107;
Nucl. Phys. B **483** (1997) 3.
- [12] J. Breitweg *et al.* [ZEUS Collaboration], Phys. Lett. B **487** (2000) 53.
- [13] A. Donnachie and P. V. Landshoff, Phys. Lett. B **296** (1992) 227.
- [14] M. Ellerbrock, these proceedings and C. Adloff *et al.* [H1 Collaboration], Eur. Phys. J. C **19** (2001) 269.
- [15] M. Moritz, these proceedings and S. Chekanov *et al.* [ZEUS Collaboration], Abstract 766, submitted to XXXIth Conf on High Energy Physics, July 2002, Amsterdam.
- [16] S. Grijpink, these proceedings and S. Chekanov *et al.* [ZEUS Collaboration], hep-ex/0205091, DESY-02-064.
- [17] F. Metlica, these proceedings.
- [18] A. M. Cooper-Sarkar, R. C. E. Devenish and A. De. Roeck, IJMPA **A 13** (1998) 3385.
- [19] A. D. Martin, R. G. Roberts, W. J. Stirling and R. S. Thorne, Eur. Phys. J. C **23** (2002) 73.
- [20] J. Pumplin, D. R. Stump, J. Huston, H. L. Lai, P. Nadolsky and W. K. Tung, JHEP **0207** (2002) 012.
- [21] R. S. Thorne, A. D. Martin, R. G. Roberts and W. J. Stirling, these proceedings, hep-ph/0207067.
- [22] W. K. Tung, these proceedings.
- [23] B. Reisert, these proceedings.
- [24] E. Tassi, these proceedings and S. Chekanov *et al.* [ZEUS Collaboration], Abstract 765, submitted to XXXIth Conf on High Energy Physics, July 2002, Amsterdam.
- [25] R. S. Thorne *et al.*, hep-ph/0205233.
- [26] A. M. Cooper-Sarkar, hep-ph/0205153.
- [27] M. Helbich, these proceedings.
- [28] U. K. Yang and A. Bodek, Phys. Rev. Lett. **84** (2000) 5456.
- [29] O. Behnke, these proceedings.
- [30] M. Prybycien, these proceedings.
- [31] A. DeRoeck, these proceedings.
- [32] S. Maxfield, these proceedings.

- [33] S.Albino, these proceedings.
- [34] P.Jankowski, these proceedings.
- [35] D. Haidt, these proceedings.
- [36] T. Lastovicka, these proceedings; [hep-ph/0203260](#).
- [37] A.V. Kotikov, these proceedings; V.G. Krikokhijine and A.V. Kotikov, [hep/0108224](#).
- [38] D.A. Timashkov, these proceedings.
- [39] S. Capitani, these proceedings, [hep-ph/0206050](#); for more details see e.g. LHPC collaboration and TXL collaboration D. Dolgov *et al.*, [hep-lat/0201021](#).
- [40] K. Golec-Biernat and M. Wüsthoff, Phys. Rev. **D59** (1999) 014017.
- [41] N. Timneanu, J. Kwiecinski and L. Motyka, these proceedings, [hep-ph/0206130](#); Eur. Phys. J. **C23** (2002) 513.
- [42] J.Bartels, K. Golec-Biernat and H. Kowalski, these proceedings, [hep-ph/0207031](#); Phys. Rev. **D66** (2002) 014001.
- [43] L. McLerran, these proceedings.
- [44] A. Freund, K. Rummukainen, H. Weigert and a Schäfer, these proceedings.
- [45] H. Weigert, Nucl. Phys. **A703** (2002) 823.
- [46] H. Jung and G.P. Salam, Eur. Phys. J. **C19** (2001) 351.
- [47] H. Jung, these proceedings [hep-ph/0207239](#).
- [48] G. Miu, these proceedings; G. Gusthafson, L. Lönnblad and G. Miu [hep-ph/0206195](#).
- [49] A.M. Stasto, these proceedings, [hep-ph/0207161](#).
- [50] M. Ciafaloni, *et al.*, [hep-ph/0204282](#).
- [51] M. Ciafaloni, *et al.*, [hep-ph/0204287](#).
- [52] S. Gieseke, these proceedings, [hep-ph/0206190](#); J. Bartels, S. Gieseke and C.F. Qiao, Phys. Rev. **D63** (2001) 056014 [Erratum -ibid. **D65** (2001) 079902]; J. Bartels, S. Gieseke and A. Kyrieleis, Phys. Rev. **D65** (2002) 014006.
- [53] S. Kretzer, these proceedings.
- [54] S. Kretzer, D. Mason and F. Olness, Phys. Rev. **D65** (2002) 074010.
- [55] W.K. Tung, S. Kretzer and C. Schmidt, J. Phys. **G28**, (2002) 983.
- [56] J. Bartels, these proceedings.
- [57] S. Moch and J.A.M. Vermaseren, these proceedings;
- [58] S. Moch and J.A.M. Vermaseren, Nucl. Phys. **B573** (2000) 853.
- [59] S.A. Larin, P. Nogueira, T. van Ritbergen and J.A.M. Vermaseren, Nucl. Phys. **B492** (1997) 338; A. Rétey and J.A.M. Vermaseren, Nucl. Phys. **B604** (2001) 281.
- [60] A.D. Martin, R.G. Roberts, W.J. Stirling and R.S. Thorne, in preparation.
- [61] A.D. Martin, R.G. Roberts, W.J. Stirling and R.S. Thorne, Phys. Lett. **B531** (2002) 216.
- [62] W.L. van Neerven and A. Vogt, Phys. Lett. **B490** (2000) 111.